Desalination and Water Treatment
www.deswater.com

doi: 10.5004/dwt.2022.28416

256 (2022) 300–313
April

Parameters optimization, kinetics, isotherm modeling of cationic and disperse dyes removal procedure using bi-polar iron electrocoagulation system

Abeer A. Moneer[a,*], Nabila M. El-Mallah[b], Manal M. El-Sadaawy[a], Mohamed Khedawy[a], Mohamed SH. Ramadan[b]

[a]*National Institute of Oceanography and Fisheries, NIOF, Egypt, emails: abeermounir30@gmail.com/ aa.moustafa@niof.sci.eg (A.A. Moneer), manal_dn@yahoo.com (M.M. El-Sadaawy), dr_khedawy@yahoo.com (M. Khedawy)*
[b]*Faculty of Science, Chemistry Department, Alexandria University, emails: dr.nabila.elmallah@gmail.com (N.M. El-Mallah), drmshafek@yahoo.com (M.S.H. Ramadan)*

Received 18 December 2021; Accepted 16 March 2022

ABSTRACT

The present work compares the efficiency of iron electrocoagulation in the removal of two different dyes; Reactive Red 35 (RR35) and Disperse Yellow 56 (DY56). Numerous operating parameters such as pH, type of supporting electrolyte were studied. The operating cost of the process was computed and it was found to be a cost-effective process in the treatment of textile wastewater. The removal of RR35 dye was under optimum conditions of 50 mg L^{-1} initial concentration, pH of 6, 0.5 g NaCl as supporting electrolyte, 43.4 A m^{-2} current density was an ideal and economic choice that gave best percent removal with maximum power saving. On the other hand, for the removal of DY56, the optimum conditions which result in the best percent removal were the same as for RR35 except for the initial dye concentration was 40 mg L^{-1}. The best removal efficiency was 96.89% and 94.67% for RR35 and DY56 respectively. Adsorption data were analyzed, different error analysis conforms that the isotherm data followed Langmuir for both studied dyes. The fact that adsorption of the dyes molecules onto the insoluble iron hydroxide flocs was established using energy-dispersive X-ray analysis and Fourier-transform infrared spectroscopy analyses. The results indicated that the first-order rate equation is the fit for the process. The thermodynamic results indicated that the process is spontaneous, randomness, and endothermic adsorption. Finally, multiple regression analyses were conducted.

Keywords: Electrocoagulation; Mechanism; Dye removal; Reactive Red 35; Disperse Yellow 56; Energy consumption; Iron electrodes; Water treatment

1. Introduction

Nowadays, ecological contamination because of industrial effluents is considered a significant issue. The textile industry expands the impressive measure of water during dyeing and finishing operations. Textile wastewater contains dyes such as reactive and disperse dyes and many other types of dyes, representing a significant ecological issue for a long time. Due to the toxicity of these synthetic compounds, they may represent a severe hazardous effect on the aquatic systems and humans [1]. Dyes from the industrial origin and even if they are with low concentrations are considered harmful materials and that's why it is essential to treat this kind of wastewater carefully before discharging into the water bodies [2]

Numerous researchers investigated several techniques for the removal of these types of pollutants, such as photocatalytic process [3], adsorption [4,5], sedimentation [6], membrane processes [7–9], biological treatment [10], and oxidation [11–13]. Furthermore, chemical coagulation, precipitation,

* Corresponding author.

electroflotation, ion exchange through a liquid-liquid membrane, membrane bioreactors, and ultrafiltration have been used also for this purpose [14]. Nevertheless, the aforementioned techniques are suffering from numerous operative drawbacks [15]. Consequently, electrochemical techniques have emerged as a solution to these problems [16].

The removal of dyes was investigated by many researchers using different techniques, which were effective to a large extent. On the other hand, these techniques were suffering from several limitations such as the high cost, the long operating time, especially for microbiological methods, and adding secondary pollution such as chemical coagulation methods [17]. The electrocoagulation (EC) technique is characterized by its simplicity, it is an economical process, and also it is favorable in most industries as a method for the treatment of its wastewater because it does not need the addition of harmful chemicals and consequently, no secondary pollution is taking place. Another important advantage is the use of low-intensity electrical current for the operation which can be obtained by solar cells, windmills, and fuel cells [16,18]. On the other hand, the EC technique suffers from some limitations such as electrode passivation, electrodes consumption, and consequently need frequent replacing, presence of metal hydroxide precipitates in the treated effluents need post-treatment. EC technique can be used as a treatment method for a variety of industrial wastewater, such as phosphates [19,20], ammonia [20], nitrates [21], organic dye molecules [22,23], arsenic [24], chromium(VI) [25], copper [26], fluoride [27,28], heavy metal ions [29], paper industry wastewater [30], and pharmaceutical wastewater [31]. Recently, EC has been investigated in the decontamination of waster as a successful method of disinfection [32].

EC technique proceeds in a three-step process as follows: firstly, oxidation reaction at the anode and reduction reaction at the cathode, secondly, formation of flocs of metal hydroxide in the bulk of the solution, and finally, adsorption of the pollutants' molecules on the surfaces of these flocs followed by aggregation of these flocs and consequently, removal of these flocs through their sedimentation or floatation according to their size and weight [33,34].

The reactions taking place at the iron anode through the EC procedure are [35]:

$$Fe_{(s)} \rightarrow Fe^{2+}_{(aq)} + 2e^{-} \quad (1)$$

The reactions for acidic and alkaline mediums are:

$$4Fe^{2+}_{(aq)} + 10H_2O_{(l)} + O_{2(g)} \rightarrow 4Fe(OH)_{3(s)} + 8H^{+}_{(aq)} \quad (2)$$

$$Fe^{2+}_{(aq)} + 2OH^{-}_{(aq)} \rightarrow Fe(OH)_{2(s)} \quad (3)$$

Water reduction is taking place at the cathode and hydrogen gas is evolved:

$$2H_2O_{(l)} + 2e^{-} \rightarrow H_{2(g)} + 2OH^{-}_{(aq)} \quad (4)$$

Among the removal mechanisms of the EC technique is the neutralization between metallic hydroxides and the pollutants which encourage their agglomeration and ease of removal [35].

The present study aimed to investigate the removal of Reactive Red 35 (RR35) and Disperse Yellow 56 (DY56) dyes from synthetic wastewater using commercial-grade iron electrodes. The literature has a little number of studies about the removal of these types of dyes particularly and using this technique specifically, that was the reason for this study. The novelty of the present work was condensed on the instrumental analyses as a professional method for the description of the removal mechanism of the dyes, which indicated the adsorption of the dyes onto the flocs. Also using different statistical analysis programs such as regression analysis and error function to ensure the results. Numerous operating factors were investigated for their effect on the percent removal of the dyes.

2. Materials and methods

2.1. Synthetic wastewater

The studied dyes named Reactive Red 35 (RR35, $C_{12}H_{18}N_3Na_3O_{14}S_4$) and Disperse Yellow 56 (DY56, $C_{21}H_{15}N_5O_2$) were acquired from Sigma-Aldrich, Germany (80% purity). Sodium sulfate (Na_2SO_4), hydrochloric acid (HCl), sodium carbonate (Na_2CO_3), sodium chloride (NaCl), sodium sulfite (Na_2SO_3), sodium acetate (CH_3COONa), and sodium hydroxide (NaOH) were obtained from Merck. All the solutions were prepared using distillate water. Iron(Fe) plates (purity: 95%, product of Egyptian Copper Company, Alexandria, Egypt) functioned as sacrificial electrodes in the EC reactor.

2.2. Instrumentations

During experimentation, the dye concentrations were analyzed using T80 UV/Vis spectrophotometer at 511 and 442 nm for RR35 and DY56, respectively. The pH meter (model AD 1030) was used for pH determination. The functional groups of the flocs were estimated by PLATINUM Diamond ATR accessory and VERTEX 70 FTIR-Bruker spectrometer. The surface characteristics and the elemental composition of the surface of electrodes and flocs before and after the removal of the dyes was estimated by energy-dispersive X-ray analysis (EDAX). The instrument was operated under a low vacuum at an accelerating voltage to achieve an adequate image of the sample.

2.3. Set-up

The dimensions and construction of the EC cell are given in Table 1. The solutions of the dyes were transferred in the reactor, a preliminary sample was taken, the anode and cathode were connected to the direct current (DC) power supply. To regulate the current and the potential of the process, an ammeter and a voltmeter (Sunwa, China) were connected to the electrodes. To achieve a homogeneous solution all along with the experiments, a magnetic stirrer was used.

The optimum conditions of the EC process are given as described in previous work [36]. The best percent removal was obtained using 9 electrodes and 0.5 g NaCl as supporting electrolytes, 2 cm as electrode's distance was optimum at all conditions and 750 rpm was optimum all over the

experiments. The optimum solution temperature was evaluated for all systems.

2.4. Analytical method

The dye adsorption capacity (Q_e, mg g^{-1}) was calculated using Eq. (5):

$$Q_e = \frac{(C_o - C_e) \times V}{W} \quad (5)$$

$$\varphi = \frac{MIt}{nF} \quad (6)$$

Table 1
Characteristics of EC reactor

Electrodes	
Material (anode and cathode)	Iron
Shape	Rectangular plate
Size (mm)	160 × 77
Number	9
Thickness(mm)	3
Plate arrangement	Parallel
Connection mode	Bipolar
Effective electrode surface area (cm^2)	123.2
Reactor characteristics	
Material	Perspex
Reactor mode	Batch
Dimensions (mm)	200 × 100 × 80
Volume (L)	1.5
Used dye volume (L)	1
Electrode gap (mm)	10
Power supply	
Voltage range (V)	0–12
Current range (A)	0–12.5

The % dye removal was determined using Eq. (7):

$$\%\text{Re} = \left(\frac{C_0 - C_t}{C_0}\right) \times 100 \quad (7)$$

3. Results and discussion

3.1. Effect of initial pH

The solution pH is among the most significant factors that control the performance of the EC technique. The pH can control the rate of anode dissolution, the state of different ions in the solution, and the speciation of coagulants [37,38]. It is also known that the acidity of the solution leads to a decline in the oxidation of Fe^{+2} to Fe^{+3} [39]. On the other hand, in the alkaline solution $Fe(OH)_4$ dominate which leads to poor coagulation [40]. Accordingly, with the presence of $Fe(OH)_3$ species, neutral and slightly alkaline mediums are preferred [41,42]. A series of experiments was performed with RR35 and DY56 aqueous solutions at various pH (2–11). As inspected in Fig. 1, the best percent removal of RR35 and DY56 was 96.89% and 91% respectively at pH 6.

This optimum pH showed that the mechanism of dyes removal by the EC process was by charging neutralization between the anionic dyes and the metallic hydroxide ions. Among the most important mechanisms of the organic pollutant removal, is the charge neutralization in which the formed flocs act as charge covering, thus, the double layer of organic pollutant is condensed then preferring the formation of coagulants leading to the precipitation [41].

3.2. Effect electrolyte type

The role of supporting electrolyte in the electrocoagulation technique is to maintain the desired conductivity of the solution, which consequently reduce the ohmic resistance of the solution. According to this reduction in the resistance, the energy consumption can be minimized [37].

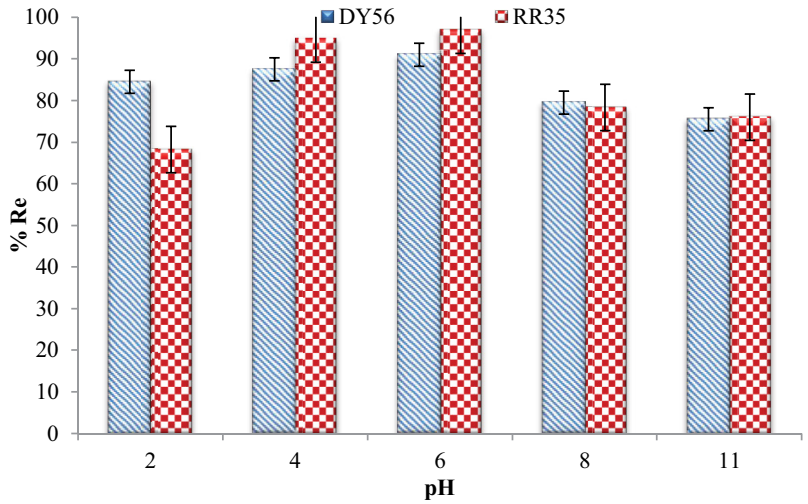

Fig. 1. Effect of pH on %Re of 50 mg L^{-1} RR35 and 40 mg L^{-1} DY56 at different initial pH values; (current density = 43.4 A m^{-2}, 0.5 g NaCl as supporting electrolyte, speed of stirring = 750 rpm, and temp. = 25°C).

Fig. 2 shows the usage of 0.5 g of different supporting electrolytes NaCl, CH_3COONa, Na_2CO_3, Na_2SO_4, and Na_2SO_3 for RR35 and DY56. It is clear that using NaCl as a supporting electrolyte gave the best percent removal for both dyes, and that Na_2SO_4 had the worst performance. The main reason for this dramatic diminution of the %Re for RR35 and DY56 with using Na_2SO_4 may be ascribed to the passivation effect of sulphate ions that retards the anode dissolution [43]. It was decided to use NaCl as a supporting electrolyte for several reasons. It is a good conductor, has a small size, is easy to ionize in the solution and it is commonly used in the textile industry for helping the absorption of the dye molecules in the fibers [44].

3.3. Thermodynamic parameters

For the investigation of the effect of temperature on the adsorption of RR35 and DY56 dye using EC processes, thermodynamic parameters named standard enthalpy change ($\Delta H°$), standard entropy change ($\Delta S°$), and standard Gibbs free energy change ($\Delta G°$) are calculated [45,46].

Table 2
Thermodynamic parameters of the RR35 and DY56 removal by EC technique

Thermodynamic parameters	Temperature (K)	RR35	DY56
$\Delta G°$ (kJ mol^{-1})	298	–7.237	–2.095
	303	–5.844	–2.968
	323	–4.732	–1.072
	343	–4.417	–0.379
$\Delta H°$ (kJ mol^{-1})		0.351	0.274
$\Delta S°$ (J mol^{-1})		9.195	1.912

Van't Hoff plot ($\ln k_d$ against $1/T$) was used for the determination of the values of the thermodynamic parameters using the intercept and slope (Table 2). When Table 2 is analyzed, it is seen that $\Delta G°$ has a negative indicating that the process is spontaneous and $\Delta H°$ has a positive value signifying the endothermic nature of the process [47]. Also, as the temperature increases, the $\Delta G°$ increases, indicating the ease of adsorption at 298 and 303 K for RR35 and DY56 respectively. Moreover, the calculated values of $\Delta G°$ ($20 < \Delta G° < 0$ kJ mol^{-1}) reveal that the dominant mechanism is a physical reaction [48,49]. The standard entropy change ($\Delta S°$) positive value displayed the randomness of the adsorption process [50,51].

3.4. Electrical energy consumption

Specific energy consumption values were calculated using Eq. (8) [52,53] with the two current densities used along with the study, which was 43.4 and 104.2 A m^{-2}.

$$\text{Electrical Energy Consumption}(\text{EEC}) = \frac{I \times v \times t}{(C_o - C_t) \times V} \quad (8)$$

Fig. 3a and b illustrate that, with the current density of 104.2 A m^{-2}, the energy consumption was much higher for both dyes. Inspecting Fig. 3c and d it can be concluded that the percent removal did not affect by the increase in current density to a great extent. Accordingly, for power saving's sake, the use of power supply 43.4 A m^{-2} was the right decision.

3.5. Operating cost

In the present study, the total operating cost (TOC) was calculated according to Eqs. (9) and (10) which include

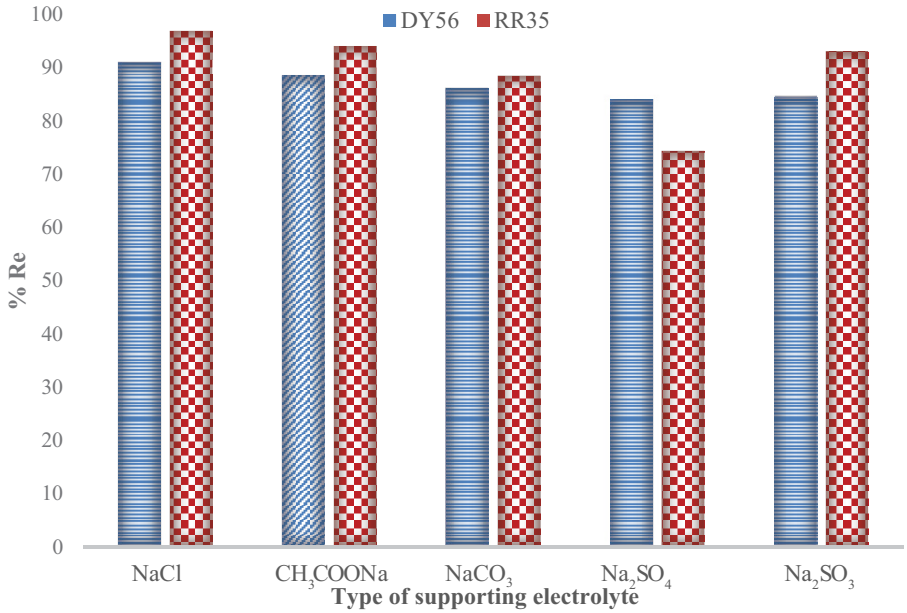

Fig. 2. The %R of RR35 and DY56 at different supporting electrolyte (0.5 g); (current density = 43.4 A m^{-2}, speed of stirring = 750 rpm, pH = 6, temp. = 25°C and initial concentration = 50 and 40 mg L^{-1} respectively).

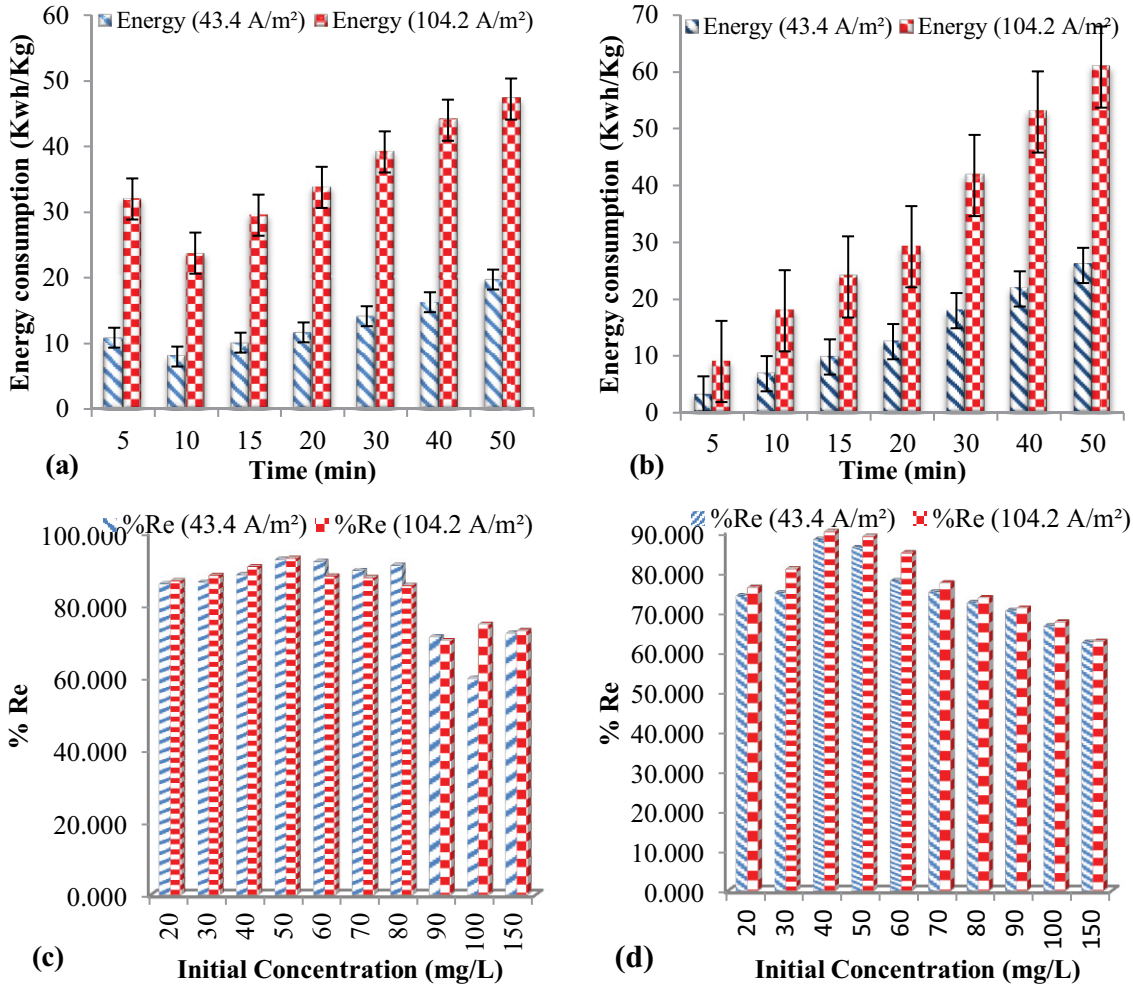

Fig. 3. Effect of different current density of 43.4 and 104.2 A m^{-2} on specific energy consumption of (a) RR35, (b) DY56 & The %Re at different current density of 43.4 and 104.2 A m^{-2} of (c) RR35, (d) DY56.

specific energy consumption (E) and cost of iron electrodes (EIC) for the evaluation of the TOC (US$/$m^3$) for real effluent [54,55]:

$$\mathrm{EIC} = \frac{I \times M_w \times t}{n \times F \times V} \tag{9}$$

$$\mathrm{TOC} = £W + ßEIC \tag{10}$$

According to the Egyptian market, during the period of the present work, June 2019, the electrical energy price for industrial sector £ and iron electrodes ß were found to be 0.05 US$/1 KWh and 0.50 US$/1 m^3, respectively. Using Eqs. (9) and (10) for calculations of operating costs led to the following results: TOC (US$/$m^3$) for real effluent for RR35 was 0.99 US$/$m^3$ and for real effluent for DY56 equal was 1.3 US$/$m^3$. For the Turkish market, in 2018 TOC for industrial estate wastewater treatment was (3.8 US$/$m^3$) [56], and in September 2015 TOC for greywater treatment was (1.64 US$/$m^3$) [57] for the Indian market, in 2021 TOC for rice grain-based distillery BDE was (1.39 US$/$m^3$) [58]. On the other hand, the operating cost for the removal of Reactive Red 223 (R223) was (4.486 $d/$m^3$) [59]. While in 2020 the total operating cost for Reactive Red 120 (RR120) (0.99 US$/$m^3$) [60]. Accordingly, the EC process is highly recommended for industrial wastewater treatment in Egypt as it is an economical technique. Table 3 presents a comparison between the obtained results from the present work with that obtained in the literature dealt with the removal of dyes with the EC technique.

3.6. Applied adsorption isotherms for EC process of RR35 and DY56 removal

The experimental data were fitted to three isotherm models, including Langmuir, Freundlich, and Temkin. The calculated parameters are shown in Table 4.

As shown in Table 4, the Langmuir isotherm model parameter (R_L) is less than unity (0.1 and 0.13) for both RR35 and DY56 respectively, confirming the favorability of the adsorption process [65,66].

As shown in Table 4, the Freundlich isotherm model parameter (n_f) is in the range of 0–10 (2.01 and 0.52 for RR35

Table 3
Comparison of optimized results with previous studies

Dye	Optimized conditions	Anode–cathode	Removal efficiency (%)	Reference
Reactive Red 35	pH = 8, 43.4 A m^{-2}, C_0 = 70 mg L^{-1}	Al–Al	95.7	[36]
Disperse Yellow 56	pH = 8, 43.4 A m^{-2}, C_0 = 50 mg L^{-1}	Al–Al	96.8	[36]
Reactive Red 231	pH = 8, 4 A m^{-2}, C_0 = 10 mg L^{-1}	Al–Al	96.5	[61]
Methyl Orange	pH = 6, 10 A m^{-2}, C_0 = 100 mg L^{-1}	Fe–Fe	92.5	[62]
Orange II	pH = 5, 2.5 A m^{-2}, C_0 = 21 mg L^{-1}	Al–Al	98	[63]
C.I. Vat Blue 1	pH = 7.5, 47 A m^{-2}, C_0 = 60 mg L^{-1}	Fe–Fe	94	[64]
Reactive Red 35	pH = 6, 43.4 A m^{-2}, C_0 = 50 mg L^{-1}	Fe–Fe	96.9	This study
Disperse Yellow 56	pH = 6, 43.4 A m^{-2}, C_0 = 40 mg L^{-1}	Fe–Fe	94.7	This study

Table 4
The calculated parameters of the used adsorption isotherm models for RR35 and DY56 removal by EC technique

Isotherm	RR35	DY56
Langmuir		
q_m (mg g^{-1})	32.26	17.39
K_a (L mg^{-1})	0.10	0.13
R_L	0.001	0.001
R^2	0.98	0.99
Freundlich		
K_f (mg g^{-1})(L $mg^{-1})^{1/n}$	1.93	1.12
n_f	2.01	0.52
R^2	0.92	0.99
Dubinin–Radushkevich		
q_m (mol g^{-1})	23.76	102
E (kJ mol^{-1})	0.010	0.010
R^2	0.86	0.87
Temkin		
b_T (mg g^{-1})	8.35	38.52
K_T (L g^{-1})	1.67	2.27
R^2	0.98	0.92

and DY56, respectively) revealing the favorable adsorption [67,68].

Temkin isotherm model parameters (A_T and b_T) are verified in Table 4. The value of the bonding factor, b_T points to the physical nature of the adsorption [48,69].

According to Table 4, the values of Dubinin–Radushkevich isotherm model parameter (E) within the range (1–8 kJ mol^{-1}) for both dyes. So, from this result, it may be concluded that adsorption can be physical adsorption of RR35 and DY56 onto the formed flocs [70].

Accordingly, the studied isotherm models can be arranged descendingly based on correlation coefficient (R^2) as follows: Langmuir > Temkin > Freundlich > Dubin in–Radushkevich and Langmuir > Freundlich > Temkin > Dubinin–Radushkevich for RR35 and DY56, respectively.

3.7. Error functions

In this study, five error functions named, root-mean-square error (RMSE), the sum of the squares of the errors (ERRSQ), mean absolute percentage error (MAPE), Marquardt's percent standard deviation (MPSD), and Chi-square analysis (χ^2) (Table 5) were applied to estimate the fit of the adsorption isotherm. The favored predictive model is that with the lower error value [71]. Table 6 illustrates the data obtained from the different models. Inspecting the table, it can be concluded that the Langmuir isotherm model best fits both studied dyes.

3.8. Kinetic studies

The adsorption mechanism was investigated using the pseudo-first-order and pseudo-second-order models [72]. Among these models, the suitable fit was selected based on statistical parameters.

The obtained results indicated that the pseudo-first-order kinetic model described accurately the adsorption process of the dyes molecules on the surface of the formed flocs with good correlation coefficients (>0.98) for both RR35 and DY56, Table 7.

3.9. Instrumental analyses of the flocs and electrodes

To prove the mechanism of the removal of the dye and whether the deposition on the electrodes or the adsorption on the flocs is responsible for the removal, EDAX analyses for the electrodes and the flocs before and after the EC process was used.

Fig. 4a and b display the EDAX analyses of the electrodes' surfaces before and after the EC process which confirms that no dyes were deposited on the electrodes' surfaces and confirms the presence of $Fe(OH)_3$ species. Accordingly, the direct $Fe(OH)_3$ deposition onto the electrodes has a minor effect on the removal of RR35 and DY56. On the other hand, the insoluble $Fe(OH)_3$ that form flocs can remove RR35 and DY56 molecules (Fig. 5a and b). This proves that the removal of the dyes depends on surface complexation between dyes and a hydrous iron moiety [73].

The Fourier-transform infrared spectroscopy (FTIR) data for the pure $Fe(OH)_3$, the flocs after RR35 and DY56 dyes

Table 5
The symbols, equations and parameters of the used error functions

Error functions	Symbol	Equation	Parameters
Sum of the squares of the errors	ERRSQ	$\sum_{i=1}^{p}\left(q_{\text{cal}}-q_e\right)_i^2$	q_{cal} and q_e are the calculated and experimental values for q (mg g^{-1})
Hybrid fractional error function	HYBRID	$\frac{100}{p-n}\sum_{i=1}^{p}\left[\frac{\left(q_e-q_{\text{cal}}\right)^2}{q_e}\right]_i$	p number of data points
Marquardt's percent standard deviation	MPSD	$100\left(\sqrt{\frac{1}{p-n}\sum_{i=1}^{p}\left[\frac{\left(q_e-q_{\text{cal}}\right)^2}{q_e}\right]_i}\right)$	n number of parameters of the isotherm equation
Average relative error	ARE	$\frac{100}{p}\sum_{i=1}^{p}\left\lvert\frac{q_{\text{cal}}-q_e}{q_e}\right\rvert_i$	
Sum of the absolute errors	EABS	$\sum_{i=1}^{p}\left\lvert q_{\text{cal}}-q_e\right\rvert_i$	

Table 6
Error function of adsorption models for the RR35 and DY56 removal by EC technique

RR35	Error function value	DY56	Error function value
Langmuir		Langmuir	
RMSE	0.046	RMSE	0.262
ERRSQ	0.78	ERRSQ	42.13
MAPE	3.6	MAPE	10.65
MPSD	16.58	MPSD	20.8
χ^2	0.18	χ^2	2.73
Freundlich		Freundlich	
RMSE	0.11	RMSE	0.53
ERRSQ	4.9	ERRSQ	63.7
MAPE	27.47	MAPE	17.28
MPSD	34.86	MPSD	29.52
χ^2	0.38	χ^2	4.67
Temkin		Temkin	
RMSE	0.47	RMSE	1.64
ERRSQ	24.3	ERRSQ	142.11
MAPE	9.47	MAPE	32.91
MPSD	20.9	MPSD	69.9
χ^2	1.14	χ^2	6.61
Dubinin–Radushkevich		Dubinin–Radushkevich	
RMSE	13.36	RMSE	3.82
ERRSQ	59.37	ERRSQ	311.28
MAPE	38.31	MAPE	175.41
MPSD	55.92	MPSD	133.63
χ^2	5.01	χ^2	16.71

removal approves the adsorption of dyes onto the insoluble iron hydroxides of the flocs. By inspecting (Fig. 6a–c); $Fe(OH)_3$ was identified by FTIR spectroscopy in the range 3,399.22–899.62 cm^{-1} for RR35 and 3,377.13–839.28 cm^{-1} for DY56, that was comparatively similar to the spectrum of a pure $Fe(OH)_{3-}$ 3,400–886 cm^{-1} [74]. The overlapping of bands of $Fe(OH)_3$ led to the shift of the absorption bands of the RR35 and DY56 spectrum from their original

Table 7
The parameters of the used kinetic models for the RR35 and DY56 removal by EC technique

Pseudo-first-order	$\log(q_e - q_t) = \log q_e - k_1 t$	k_1 (min^{-1}) = 0.053 R^2 = 0.982	k_1 (min^{-1}) = 0.097 R^2 = 0.99
Pseudo-second-order	$\frac{t}{q_t} = \frac{1}{k_2 q_e^2} + \frac{t}{q_e}$	k_2 (g mg^{-1} min^{-1}) = 0.015 R^2 = 0.954	k_2 (g mg^{-1} min^{-1}) = 0.015 R^2 = 0.953

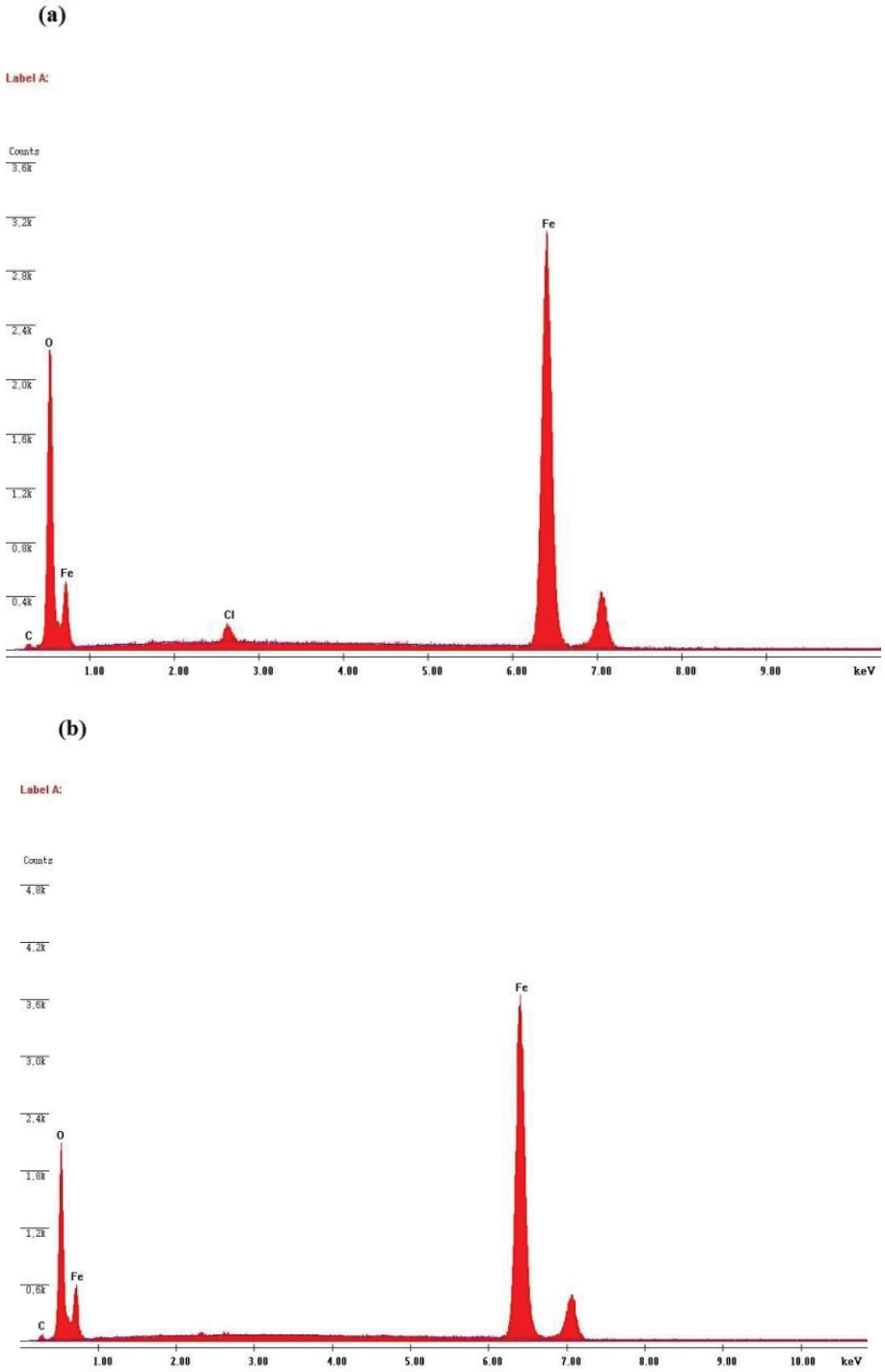

Fig. 4. EDAX of Fe electrodes' surface: (a) before and (b) after dyes removal by EC technique.

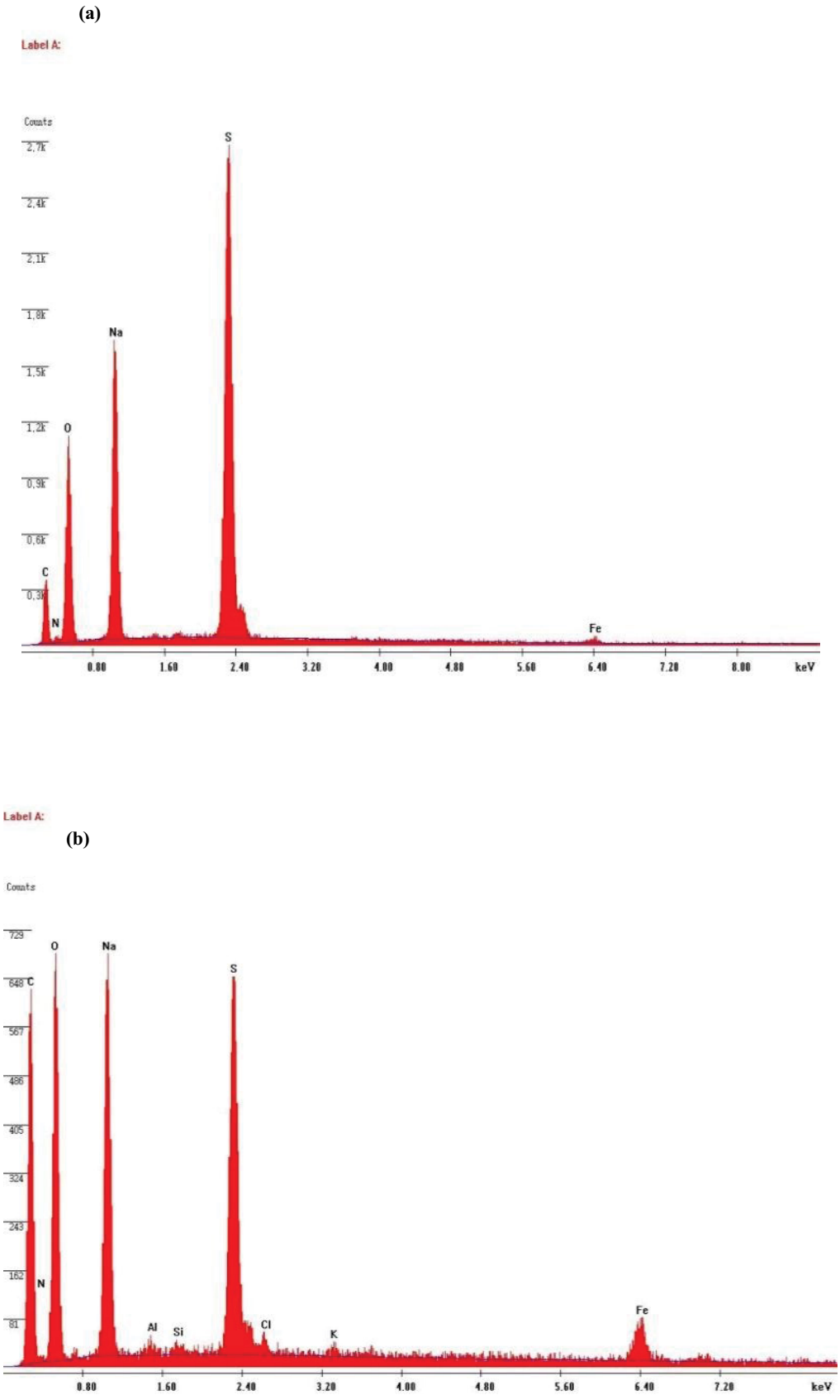

Fig. 5. EDAX of the formed flocs after (a) RR35 and (b) DY56 removal by EC technique using Fe electrode.

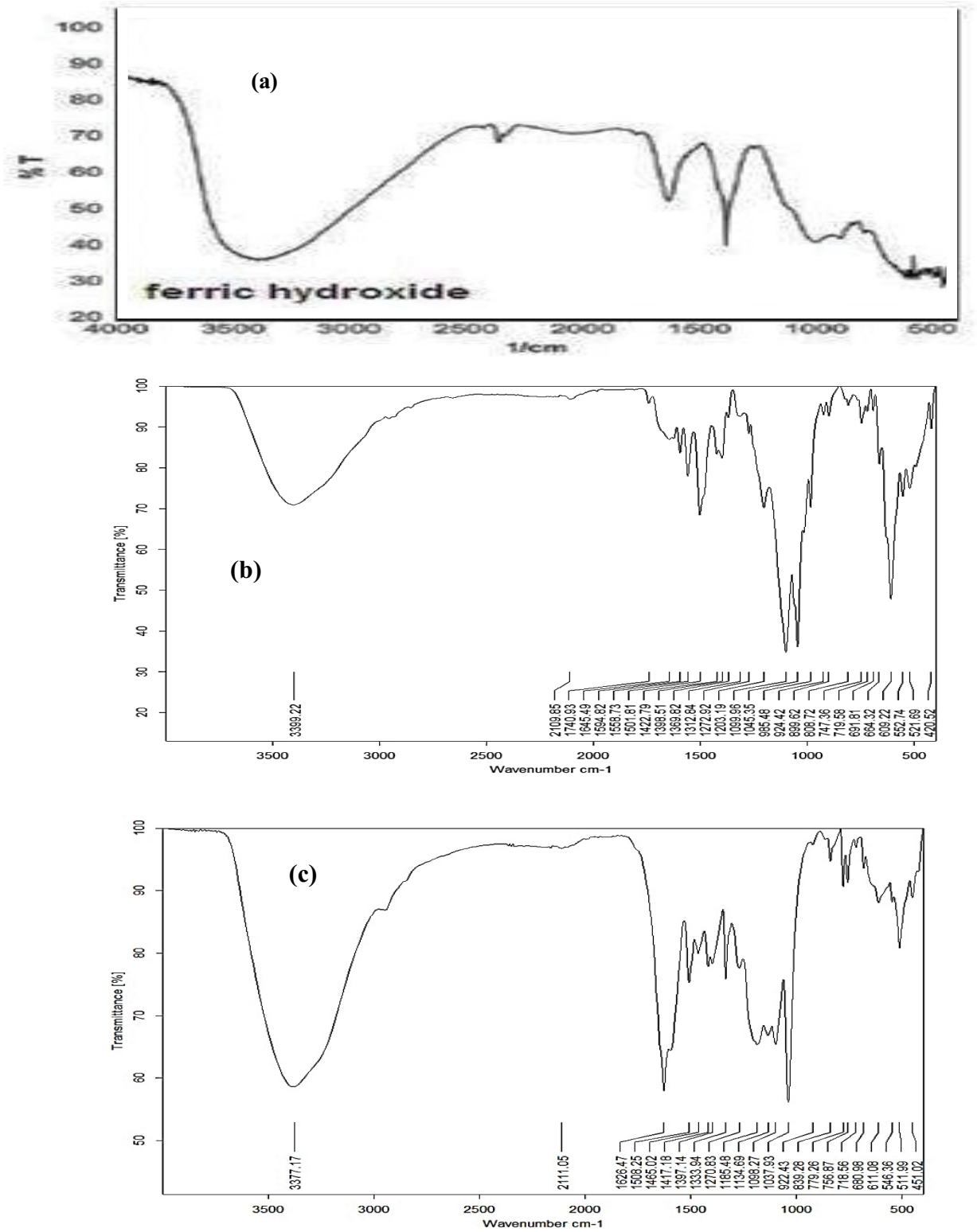

Fig. 6. FTIR of the formed flocs of (a) pure ferric hydroxide, (b) flocs formed of RR35 removal and (c) flocs formed of DY56 removal by EC technique using Fe electrodes.

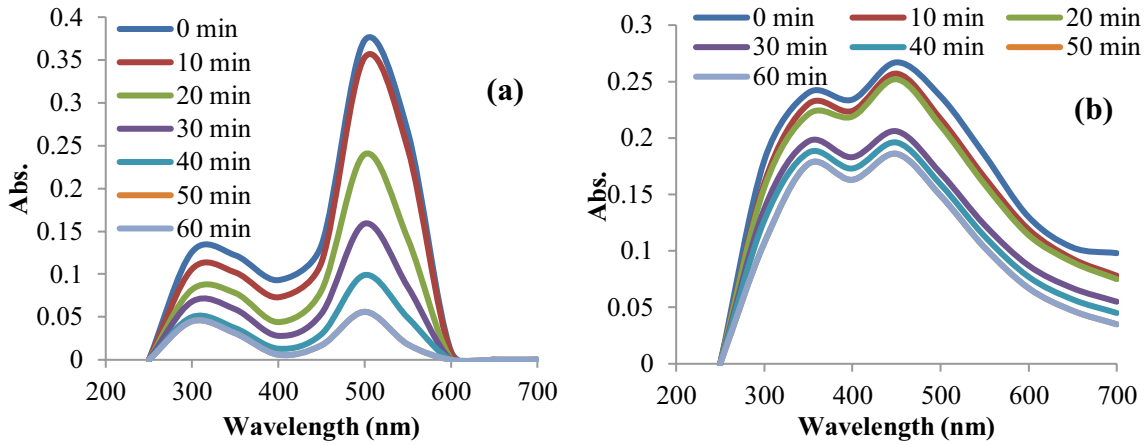

Fig. 7. Absorption spectra for (a) RR35 and (b) DY56 using Fe electrodes of electrocoagulation.

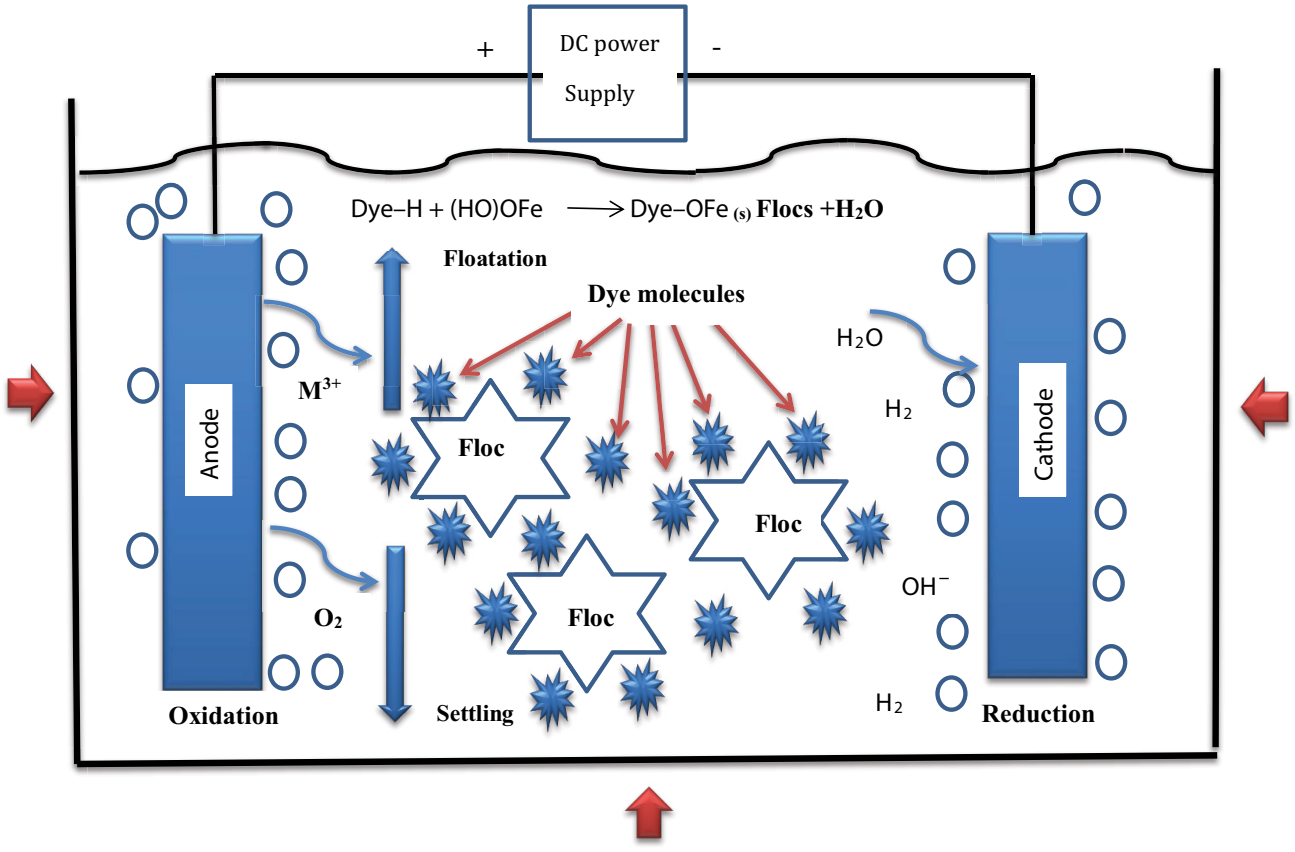

Fig. 8. Schematic diagram of dyes removal mechanism by electrocoagulation technique.

positions for the pure composition [75]. However, N–H stretching vibrations were assigned by bands at 3,399.22 and 3,377.17 cm^{-1} for RR35 and DY56 respectively. The benzene rings were found at peaks 1,594.82 and 1,465.02 cm^{-1} for RR35 and DY56 respectively. For the C=C stretching, peaks at 1,501.81 and 1,508.25 cm^{-1} for N=N stretching [76]. The peaks at 1,099.96 and 1,037.93 cm^{-1} referred to C–OH bending vibrations and a peak at 609.22 and 611.08 cm^{-1} corresponds to the C–Cl stretching vibrations. There has been more than one peak found in the area of the C–H bending vibrations (985.48–420.52 cm^{-1}) that could support the presence of an aromatic structure.

3.10. Absorption spectra analysis

To discuss the mechanism of dye removal, the UV-VIS spectra of the dye solutions collected at 0–60 min of the EC process were investigated (Fig. 7a and b). It was shown

that before treatment the dyes RR35 and DY56 were described by one principal band in the visible area with a peak of 500 and 450 nm, respectively. Another band in the ultraviolet region with a peak at 300 nm for RR35 and 350 nm for DY56. The bands in the visible region from 400 nm to around 500 nm and the bands in the ultraviolet region around 300–390 could be assigned to the n–π^* transition of the (N=N) group and the π–π^* transition related to the aromatic ring attached to the (N=N) group in the dye molecule, respectively [77].

Inspecting Fig. 7a and b, it is clear that complete removal of the dyes using EC technique was taking place, and no dissociation of the dyes molecules and no intermediates were formed during the process which may cause secondary pollution.

3.11. Multiple regression analyses

IBM SPSS STATISTICA 22 was used to conduct the multiple regression analyses. Multiple regression hypothetical equations were formulated using dependent variables of the percent removal of the dyes; under independent variables of pH, electrolysis time (min), initial concentration (mg L^{-1}), concentrations at time t (C_t), electrodes consumption (g) at constant temperature (25°C ± 2°C). The resultant multiple regression report concerning the high significant predicted equation (R = 0.91 and 0.95 for DY65 and RR35, respectively). The hypothetical equation can be illustrated as follows:

$$\begin{aligned}\text{Re}\% &= 106.97 + 0.267\ \text{contact time} + 0.469C_0 \\ &\quad - 0.76C_t + 0.267\ \text{Fe coagulate} - 0.32\ \text{pH} \\ &\quad \left(R = 0.91, P < 0.000\right) \text{for DY65}\end{aligned} \tag{11}$$

and

$$\begin{aligned}\text{Re}\% &= -29.579 + 0.084C_0 - 0.353C_t \\ &\quad + 0.534\ \text{Fe coagulate} + 0.329\ \text{pH} \\ &\quad \left(R = 0.95, P < 0.000\right) \text{for RR35}\end{aligned} \tag{12}$$

3.12. Mechanism of dyes removal

The adsorption of the dye molecules on the produced flocs of iron hydroxide gelatinous suspension by charge neutralization between iron hydroxide and the functional groups of the dye molecules is seen in Fig. 8; according to Eq. (13).

$$\text{Dye} - \text{H}_{(\text{aq})} + \left(\text{OH}\right)\text{OM}_{(\text{s})} \rightarrow \text{Dye} - \text{OM}_{(\text{s})} + \text{H}_2\text{O}_{(\text{l})} \tag{13}$$

Furthermore, by examining the various adsorption isotherms, it was shown that the monolayer adsorption model (the Langmuir adsorption isotherm model) better explained both RR35 and DY56 adsorption.

4. Conclusions

Numerous operation parameters were studied for a comparison between the behavior of RR35 and DY56 dyes in the treatment by Fe electrocoagulation technique in a step forward for the recommendation of this technique to the industrial wastewater treatment. These parameters were pH, type of supporting electrolyte. It was concluded that removal of RR35 dye was under optimum conditions of 50 mg L^{-1} initial concentration, 43.4 A m^{-2} current density was an ideal and economic choice that gave best percent removal with maximum power saving. A pH of 6, 0.5 g NaCl as supporting electrolyte. On the other hand, for the removal of DY56, the optimum conditions which result in the best percent removal were the same as for RR35 except for the initial dye concentration was 40 mg L^{-1}. Different instrumental analyses (EDAX and FTIR) were performed to explain the behavior of dyes removal, they significantly proved the removal of RR35 and DY56 from the bulk solution by its adsorption on the insoluble iron hydroxides of the flocs in a short time. Both RR35 and DY56 adsorption were best fitted by the monolayer adsorption model (the Langmuir adsorption isotherm). The kinetic study indicated that the dyes were adsorbed on iron hydroxide flocs was best described using the pseudo-first-order kinetic model. The absorption spectra analysis of the two dyes indicated that dyes degradation is not taking place during the EC process. STATISTICA 6.0. was employed for the correlation matrix and multiple regression analyses for different variables including, initial pH, contact time, initial and interval concentrations, %Re, and mass of Fe coagulant.

References

[1] S. Li, Z. Zeng, W. Xue, Kinetic and equilibrium study of the removal of reactive dye using modified walnut shell, Water Sci. Technol., 80 (2019) 874–883.
[2] A.G. Khorram, N. Fallah, Treatment of textile dyeing factory wastewater by electrocoagulation with low sludge settling time: optimization of operating parameters by RSM, J. Environ. Chem. Eng., 6 (2018) 635–642.
[3] P.V. Nidheesh, R. Gandhimathi, Effect of solution pH on the performance of three electrolytic advanced oxidation processes for the treatment of textile wastewater and sludge characteristics, RSC Adv., 4 (2014) 27946–27954.
[4] G.K. Sarma, S.S. Gupta, K.G. Bhattacharyya, Removal of hazardous basic dyes from aqueous solution by adsorption onto kaolinite and acid-treated kaolinite: kinetics, isotherm and mechanistic study, SN Appl. Sci., 1 (2019) 211, doi: 10.1007/s42452-019-0216-y.
[5] Z. Berizi, S.Y. Hashemi, M. Hadi, A. Azari, A.H. Mahvi, The study of non-linear kinetics and adsorption isotherm models for Acid Red 18 from aqueous solutions by magnetite nanoparticles and magnetite nanoparticles modified by sodium alginate, Water Sci. Technol., 74 (2016) 1235–1242.
[6] B.K. Nandi, A. Goswami, M.K. Purkait, Adsorption characteristics of brilliant green dye on kaolin, J. Hazard. Mater., 161 (2009) 387–395.
[7] M.R. Bilad, P. Declerck, A. Piasecka, L. Vanysacker, X. Yan, I.F.J. Vankelecom, Treatment of molasses wastewater in a membrane bioreactor: influence of membrane pore size, Sep. Purif. Technol., 78 (2011) 105–112.
[8] M. Rezayi, R. Karazhian, Y. Abdollahi, L. Narimani, S.B.T. Sany, S. Ahmadzadeh, Y. Alias, Titanium(III) cation selective electrode based on synthesized tris(2pyridyl) methylamine ionophore and its application in water samples, Sci. Rep., 41 (2014) 4664, doi: 10.1038/srep04664.
[9] M. Rezayi, L.Y. Heng, A. Kassim, S. Ahmadzadeh, Y. Abdollahi, H. Jahangirian, Immobilization of tris(2 pyridyl) methylamine in a PVC-membrane sensor and characterization of the membrane properties, Chem. Cent. J., 6 (2012) 40, doi: 10.1186/1752-153X-6-40..

[10] H.S. Rai, M.S. Bhattacharyya, J. Singh, T.K. Bansal, P. Vats, U.C. Banerjee, Removal of dyes from the effluent of textile and dyestuff manufacturing industry: a review of emerging techniques with reference to biological treatment, Crit. Rev. Env. Sci. Technol., 35 (2005) 219–238.
[11] M.A. Hassaan, A. El Nemr, F.F. Madkour, Advanced oxidation processes of Mordant Violet 40 dye in freshwater and seawater, Egypt. J. Aquat. Res., 43 (2017a) 1–9.
[12] M.A. Hassaan, A. El Nemr, F.F. Madkour, Testing the advanced oxidation processes on the degradation of Direct Blue 86 dye in wastewater, Egypt. J. Aquat. Res., 43 (2017b) 11–19.
[13] M. Dolatabadi, T. Świergosz, S. Ahmadzadeh, Electro-Fenton approach in oxidative degradation of dimethyl phthalate – the treatment of aqueous leachate from landfills, Sci. Total Environ., 772 (2021) 145323, doi: 10.1016/j.scitotenv.2021.145323.
[14] M.K. Mbacké, C. Kane, N.O. Diallo, C.M. Diop, F. Chauvet, M. Comtat, T. Tzedakis, Electrocoagulation process applied on pollutants treatment-experimental optimization and fundamental investigation of the crystal violet dye removal, J. Environ. Chem. Eng., 4 (2016) 4001–4011.
[15] B. Khemila, B. Merzouk, A. Chouder, R. Zidelkhir, J.P. Leclerc, F. Lapicque, Removal of a textile dye using photovoltaic electrocoagulation, Sustainable Chem. Pharm., 7 (2018) 27–35.
[16] E. Brillas, C.A. Martínez-Huitle, Decontamination of wastewaters containing synthetic organic dyes by electrochemical methods. An updated review, Appl. Catal., B, 166–167 (2015) 603–643.
[17] M. Suzuki, Y. Suzuki, K. Uzuka, Y. Kawase, Biological treatment of non-biodegradable azo-dye enhanced by zero-valent iron (ZVI) pre-treatment, Chemosphere, 259 (2020) 127470, doi: 10.1016/j.chemosphere.2020.127470.
[18] L. Ayhan Şengil, A. Özdemir, Simultaneous decolorization of binary mixture of blue disperse and yellow basic dyes by electrocoagulation, Desal. Water Treat., 46 (2012) 215–226.
[19] A. Dura, C.B. Breslin, Electrocoagulation using stainless steel anodes: simultaneous removal of phosphates, Orange II and zinc ions, J. Hazard. Mater., 374 (2019) 152–158.
[20] D. Sun, X. Hong, K. Wu, K.S. Hui, Y. Du, K.N. Hui, Simultaneous removal of ammonia and phosphate by electro-oxidation and electrocoagulation using RuO_2–IrO_2/Ti and microscale zero-valent iron composite electrode, Water Res., 169 (2020) 115239, doi: 10.1016/j.watres.2019.115239.
[21] D. Xu, Y. Li, L. Yin, Y. Ji, J. Niu, Y. Yu, Electrochemical removal of nitrate in industrial wastewater, Front. Environ. Sci. Eng., 12 (2018) 1–14, doi: 10.1007/s11783-018-1033-z.
[22] M. Chafi, B. Gourich, A.H. Essadki, C. Vial, A. Fabregat, Comparison of electrocoagulation using iron and aluminium electrodes with chemical coagulation for the removal of a highly soluble acid dye, Desalination, 281 (2011) 285–292.
[23] A.A. Moneer, M.M. El-Sadaawy, G.F. El-Said, F.A.M. Morsy, Modeling adsorption kinetic of crystal violet removal by electrocoagulation technique using bipolar iron electrodes, Water Sci. Technol., 77 (2018) 323–336.
[24] N.S. Kumar, S. Goel, Factors influencing arsenic and nitrate removal from drinking water in a continuous flow electrocoagulation (EC) process, J. Hazard. Mater., 173 (2010) 528–533.
[25] S. Aoudj, A. Khelifa, N. Drouiche, R. Belkada, D. Miroud, Simultaneous removal of chromium(VI) and fluoride by electrocoagulation-electroflotation: application of a hybrid Fe-Al anode, Chem. Eng. J., 267 (2015) 153–162.
[26] A.A. Moneer, A.A. El-Shafei, M.M. Elewa, M.M. Naim, Removal of copper from simulated wastewater by electrocoagulation/floatation technique, Desal. Water Treat., 57 (2016) 22824–22834.
[27] R. Mureth, R. Machunda, K.N. Njau, D. Dodoo-Arhin, Assessment of fluoride removal in a batch electrocoagulation process: a case study in the Mount Meru Enclave, Sci. Afr., 12 (2021) e00737, doi: 10.1016/j.sciaf.2021.e00737.
[28] M.M. Naim, A.A. Moneer, G.F. El-Said, Defluoridation of commercial and analar sodium fluoride solutions without using additives by batch electrocoagulation-flotation technique, Desal. Water Treat., 44 (2012) 110–117.
[29] M. Al-Shannag, Z. Al-Qodah, K. Bani-Melhem, M.R. Qtaishat, M. Alkasrawi, Heavy metal ions removal from metal plating wastewater using electrocoagulation: kinetic study and process performance, Chem. Eng. J., 260 (2015) 749–756.
[30] A. Barhoumi, S. Ncib, A. Chibani, K. Brahmi, W. Bouguerra, E. Elaloui, High-rate humic acid removal from cellulose and paper industry wastewater by combining electrocoagulation process with adsorption onto granular activated carbon, Ind. Crops Prod., 140 (2019) 111715, doi: 10.1016/j.indcrop.2019.111715.
[31] B.K. Zaied, M. Rashid, M. Nasrullah, A.W. Zularisam, D. Pant, L. Singh, A comprehensive review on contaminants removal from pharmaceutical wastewater by electrocoagulation process, Sci. Total Environ., 726 (2020) 138095, doi: 10.1016/j.scitotenv.2020.138095.
[32] N. Boudjema, N. Drouiche, M. Kherat, N. Mameri, Wastewater disinfection by electrocoagulation process and its interaction with abiotic parameters, Desal. Water Treat., 57 (2016) 28151–28159.
[33] A.I. Adeogun, R.B. Balakrishnan, Kinetics, isothermal and thermodynamics studies of electrocoagulation removal of basic dye Rhodamine B from aqueous solution using steel electrodes, Appl. Water Sci., 7 (2017) 1711–1723.
[34] S. Bener, Ö. Bulca, B. Palas, G. Tekin, S. Atalay, G. Ersöz, Electrocoagulation process for the treatment of real textile wastewater: effect of operative conditions on the organic carbon removal and kinetic study, Process Saf. Environ. Prot., 129 (2019) 47–54.
[35] J. Núñez, M. Yeber, N. Cisternas, R. Thibaut, P. Medina, C. Carrasco, Application of electrocoagulation for the efficient pollutants removal to reuse the treated wastewater in the dyeing process of the textile industry, J. Hazard. Mater., 371 (2019) 705–711.
[36] A.A. Moneer, N.M. El-Mallah, M.M. El-Sadaawy, M. Khedawy, M.S.H. Ramadan, Kinetics, thermodynamics, isotherm modeling for removal of Reactive Red 35 and Disperse Yellow 56 dyes using batch bi-polar aluminum electrocoagulation, Alexandria Eng. J., 60 (2021) 4139–4154.
[37] R. Keyikoglu, O.T. Can, A. Aygun, A. Tek, Comparison of the effects of various supporting electrolytes on the treatment of a dye solution by electrocoagulation process, Colloids Interface Sci. Commun., 33 (2019) 100210, doi: 10.1016/j.colcom.2019.100210.
[38] M. Fouladgar, S. Ahmadzadeh, Application of a nanostructured sensor based on NiO nanoparticles modified carbon paste electrode for determination of methyldopa in the presence of folic acid, Appl. Surf. Sci., 379 (2016) 150–155.
[39] C. Escobar, C. Soto-Salazar, M. Inés Toral, Optimization of the electrocoagulation process for the removal of copper, lead and cadmium in natural waters and simulated wastewater, J. Environ. Manage., 81 (2006) 384–391.
[40] C. Jiménez, C. Sáez, F. Martínez, P. Cañizares, M.A. Rodrigo, Electrochemical dosing of iron and aluminum in continuous processes: a key step to explain electro-coagulation processes, Sep. Purif. Technol., 98 (2012) 102–108.
[41] S. Garcia-Segura, M.M.S.G. Eiband, J.V. de Melo, C.A. Martínez-Huitle, Electrocoagulation and advanced electrocoagulation processes: a general review about the fundamentals, emerging applications and its association with other technologies, J. Electroanal. Chem., 801 (2017) 267–299.
[42] W.T. Mook, M.K. Aroua, M. Szlachta, C.S. Lee, Optimisation of Reactive Black 5 dye removal by electrocoagulation process using response surface methodology, Water Sci. Technol., 75 (2017) 952–962.
[43] S.I. Pyun, S.M. Moon, S.H. Ahn, S.S. Kim, Effects of Cl^-, NO_3^- and SO_4^{2-} ions on anodic dissolution of pure aluminum in alkaline solution, Corros. Sci., 41 (1999) 653–667.
[44] D.T. Cestarolli, A. das Graças de Oliveira, E.M. Guerra, Removal of Eriochrome Black textile dye from aqueous solution by combined electrocoagulation–electroflotation methodology, Appl. Water Sci., 9 (2019) 101, doi: 10.1007/s13201-019-0985-x.
[45] G.H. Rounaghi, M. Mohajeri, S. Ahmadzadeh, S. Tarahomi, A thermodynamic study of interaction of Na^+ cation with benzo-15-crown-5 in binary mixed non-aqueous solvents, J. Inclusion Phenom. Macrocyclic Chem., 63 (2009) 365–372.

[46] S. Ahmadzadeh, M. Rezayi, H. Karimi-Maleh, Y. Alias, Conductometric measurements of complexation study between 4-Isopropylcalix[4]arene and Cr^{3+} cation in THF–DMSO binary solvents, Measurement, 70 (2015) 214–224.
[47] T. Bayram, S. Bucak, D. Ozturk, BR13 dye removal using sodium dodecyl sulfate modified montmorillonite: equilibrium, thermodynamic, kinetic and reusability studies, Chem. Eng. Process. Process Intensif., 158 (2020) 108186, doi: 10.1007/s13201-019-0985-x.
[48] A.H. Shobier, M.M. El-Sadaawy, G.F. El-Said, Removal of hexavalent chromium by ecofriendly raw marine green alga *Ulva fasciata*: kinetic, thermodynamic and isotherm studies, Egypt. J. Aquat. Res., 46 (2020) 325–331.
[49] N.S. Al-Kadhi, The kinetic and thermoynamic study of the adsorption Lissamine Green B dye by micro-particle of wild plants from aqueous solutions, Egypt. J. Aquat. Res., 45 (2019) 231–238.
[50] A.H. Jawad, A.S. Abdulhameed, M.S. Mastuli, Mesoporous crosslinked chitosan-activated charcoal composite for the removal of thionine cationic dye: comprehensive adsorption and mechanism study, J. Polym. Environ., 28 (2020) 1095–1105.
[51] A.H. Jawad, I.A. Mohammed, A.S. Abdulhameed, Tuning of fly ash loading into chitosan-ethylene glycol diglycidyl ether composite for enhanced removal of Reactive Red 120 dye: optimization using the Box–Behnken design, J. Polym. Environ., 28 (2020) 2720–2733.
[52] B.N. Patil, D.B. Naik, V.S. Shrivastava, Photocatalytic degradation of hazardous Ponceau-S dye from industrial wastewater using nanosized niobium pentoxide with carbon, Desalination, 269 (2011) 276–283.
[53] R. Niazmand, M. Jahani, F. Sabbagh, S. Rezania, Optimization of electrocoagulation conditions for the purification of table olive debittering wastewater using response surface methodology, Water, 12 (2020) 1687, doi: 10.3390/w12061687.
[54] F. Ulu, S. Barişçi, M. Kobya, M. Sillanpää, An evaluation on different origins of natural organic matters using various anodes by electrocoagulation, Chemosphere, 125 (2015) 108–114.
[55] M. Taheri, M.R. Alavi Moghaddam, M. Arami, Optimization of Acid Black 172 decolorization by electrocoagulation using response surface methodology, J. Environ. Health Sci. Eng., 9 (2012) 18–20.
[56] Y. Yavuz, B. Ögütveren, Treatment of industrial estate wastewater by the application of electrocoagulation process using iron electrodes, J. Environ. Manage., 207 (2018) 151–158.
[57] S. Barişçi, O. Turkay, Domestic greywater treatment by electrocoagulation using hybrid electrode combinations, J. Water Process Eng., 10 (2016) 56–66.
[58] A.K. Prajapati, Sono-assisted electrocoagulation treatment of rice grain based distillery biodigester effluent: performance and cost analysis, Process Saf. Environ. Prot., 150 (2021) 314–322.
[59] A.R. Shah, H. Tahir, H.M.K. Ullah, A. Adnan, Optimization of electrocoagulation process for the removal of binary dye mixtures using response surface methodology and estimation of operating cost, Open J. Appl. Sci., 7 (2017) 458–484.
[60] K. Gautam, S. Kamsonlian, S. Kumar, Removal of Reactive Red 120 dye from wastewater using electrocoagulation: optimization using multivariate approach, economic analysis, and sludge characterization, Sep. Sci. Technol. (Philadelphia), 55 (2020) 3412–3426.
[61] C.E. Lach, C.S. Pauli, A.S. Coan, E.L. Simionatto, L.A.D Koslowski, Investigating the process of electrocoagulation in the removal of azo dye from synthetic textile effluents and the effects of acute toxicity on *Daphnia magna* test organisms, J. Water Process Eng., 45 (2022) 102485, doi: 10.1016/j.jwpe.2021.102485.
[62] Z. Wu, J. Dong, Y. Yao, Y. Yang, F. Wei, Continuous flowing electrocoagulation reactor for efficient removal of azo dyes: kinetic and isotherm studies of adsorption, Environ. Technol. Innovation, 22 (2021) 101448, doi: 10.1016/j.eti.2021.101448.
[63] S.C.M. Signorelli, J.M. Costa, A.F.de. Almeida Neto, Electrocoagulation-flotation for Orange II dye removal: kinetics, costs, and process variables effects, J. Environ. Chem. Eng., 9 (2021) 106157, doi: 10.1016/j.jece.2021.106157.
[64] K. Hendaoui, M. Trabelsi-Ayadi, F. Ayari, Optimization and mechanisms analysis of indigo dye removal using continuous electrocoagulation, Chin. J. Chem. Eng., 29 (2021) 242–252.
[65] M.A. Al-Ghouti, D.A. Da'ana, Guidelines for the use and interpretation of adsorption isotherm models: a review, J. Hazard. Mater., 393 (2020) 122383, doi: 10.1016/j.jhazmat.2020.122383.
[66] M. Heydari Moghaddam, R. Nabizadeh, M.H. Dehghani, B. Akbarpour, A. Azari, M. Yousefi, Performance investigation of Zeolitic Imidazolate Framework-8 (ZIF-8) in the removal of trichloroethylene from aqueous solutions, Microchem. J., 150 (2019) 104185, doi: 10.1016/j.microc.2019.104185.
[67] M. El Ouardi, M. Laabd, H. Abou Oualid, Y. Brahmi, A. Abaamrane, A. Elouahli, A. Ait Addi, A. Laknifli, Efficient removal of p-nitrophenol from water using montmorillonite clay: insights into the adsorption mechanism, process optimization, and regeneration, Environ. Sci. Pollut. Res., 26 (2019) 19615–19631.
[68] Y. Rashtbari, S. Hazrati, A. Azari, S. Afshin, M. Fazlzadeh, M. Vosoughi, A novel, eco-friendly and green synthesis of PPAC-ZnO and PPAC-nZVI nanocomposite using pomegranate peel: cephalexin adsorption experiments, mechanisms, isotherms and kinetics, Adv. Powder Technol., 4 (2020) 1612–1623.
[69] E. Ahmadi, B. Kakavandi, A. Azari, H. Izanloo, H. Gharibi, A.H. Mahvi, A. Javid, S.Y. Hashemi, The performance of mesoporous magnetite zeolite nanocomposite in removing dimethyl phthalate from aquatic environments, Desal. Water Treat., 57 (2016) 27768–27782.
[70] I. Hamadneh, R.A. Abu-Zurayk, A.H. Al-Dujaili, Removal of phenolic compounds from aqueous solution using MgC_{12}-impregnated activated carbons derived from olive husk: the effect of chemical structures, Water Sci. Technol., 81 (2020) 2351–2367.
[71] A. Terdputtakun, O.-a. Arqueropanyo, P. Sooksamiti, S. Janhom, W. Naksata, Adsorption isotherm models and error analysis for single and binary adsorption of Cd(II) and Zn(II) using leonardite as adsorbent, Environ. Earth Sci., 76 (2017) 777.
[72] M. Dolatabadi, M.T. Ghaneian, C. Wang, S. Ahmadzadeh, Electro-Fenton approach for highly efficient degradation of the herbicide 2,4-dichlorophenoxyacetic acid from agricultural wastewater: process optimization, kinetic and mechanism, J. Mol. Liq., 334 (2021) 116116, doi: 10.1016/j.molliq.2021.116116.
[73] N. Daneshvar, A. Oladegaragoze, N. Djafarzadeh, Decolorization of basic dye solutions by electrocoagulation: an investigation of the effect of operational parameters, J. Hazard. Mater., 129 (2006) 116–122.
[74] S. Mustafa, M. Irshad, M. Waseem, K.H. Shah, U. Rashid, W. Rehman, Adsorption of heavy metal ions in ternary systems onto $Fe(OH)_3$, Korean J. Chem. Eng., 30 (2013) 2235–2240.
[75] M.F.H. Al-Kadhemy, Z.S. Rasheed, S.R. Salim, Fourier transform infrared spectroscopy for irradiation coumarin doped polystyrene polymer films by alpha ray, J. Radiat. Res. Appl. Sci., 9 (2016) 321–331.
[76] R. Hosoda, N. Kamoshida, N. Hoshi, Y. Einaga, M. Nakamura, In situ infrared spectroscopy of dopamine oxidation/reduction reactions on a polycrystalline boron-doped diamond electrode, Carbon, 171 (2021) 814–818.
[77] M. Saravanan, N.P. Sambhamurthy, M. Sivarajan, Treatment of Acid blue 113 dye solution using iron electrocoagulation, Clean – Soil, Air, Water, 38 (2010) 565–571.